Ordering of amorphous silicon during solid-phase epitaxy studied by scanning tunneling microscopy

E. Ter-Ovanesyan, Y. Manassen, and D. Shachal
Department of Chemical Physics, Weizmann Institute of Science, Rehovot 76100, Israel
(Received 21 March 1994)

The early stages of silicon solid-phase epitaxy (SPE) on the Si(111) surface are studied by scanning tunneling microscopy (STM). It is shown that an amorphous layer with thickness around two bilayers deposited on the silicon surface transforms in a polycrystalline layer with extremely small grain size (about 2–3 nm) after heating to 430 °C. The atomic-resolution STM imaging of such a disordered surface allows us to extract lateral coordinates of the upper-layer atoms. The application of the pair-distribution-function formalism reveals anisotropy in the orientational order that might indicate that the SPE occurs preferably in the step direction.

It is known that an amorphous-silicon (*a*-Si) layer on a crystalline silicon surface is crystallized epitaxially at relatively low temperatures (550 °C–600 °C). This process known as solid-phase epitaxy (SPE) has been extensively studied by many different techniques.[1–4] The growth rate is the main SPE quantity measured as a function of temperature, pressure, substrate orientation, doping, etc. It is well established that the growth rate is constant at isothermal annealing and it is described by Arrhenius dependence with an activation energy of 2.7 eV.[3] Such behavior is characteristic for interface-controllable processes.[2] However, more experimental microscopic data about the interface structure are needed in order to understand the atomic mechanism of SPE and the origin of SPE activation energy. Such data can be obtained from a scanning tunneling microscopy (STM) study of the surface when the amorphous-crystalline interface reaches it. Although STM images of amorphous silicon show general topography without atomic resolution,[4,5] STM can provide atomically resolved information on real structures lacking long-range order. An example is images of partly disordered Si(111) surfaces.[6,7]

A STM study of the early stages of SPE on the Si(111) surface is reported here. It is shown that SPE of two bilayers of vacuum-deposited *a*-Si at rather low temperatures produces a surface with extremely small grain size (2–3 nm). The rather sharp atomic resolution in the resulting layer enables the determination of the lateral coordinates of atoms. Pair-distribution functions $g(r)$ and $G(\mathbf{r})$ were calculated to characterize the order in a quantitative way. The notation $G(\mathbf{r})$ is used here for the normalized probability of finding two atoms with the scalar distance r in a direction $\mathbf{r}/r$. $g(r)$ is the average of $G(\mathbf{r})$ over all directions.[8] While $g(r)$ (for large samples) can be obtained from x-ray experiments,[9–11] $G(\mathbf{r})$ is calculated so far for models only. A comparison of the intensities of the first-neighbor peaks in $G(\mathbf{r})$ reveals a larger degree of orientational order along the step direction. We believe that it means that SPE occurs preferably along this direction.

The experiments were performed in an ultrahigh vacuum chamber (base pressure 2×10^{-10} Torr) containing a "Demuth-type" home-built STM,[12] low-energy electron diffraction (LEED), and an electron-beam evaporator. The sample was a Sb-doped Si(111) wafer of 0.01–0.02 Ω cm that was cleaned *in situ* by thermally removing the native oxide at 900 °C with subsequent short flash at 1000 °C. After cooling for 2 h the sample was transferred to the STM to verify the quality of the (7×7) reconstructed surface. Then two bilayers (one bilayer equals 2 ML, which equals 1.56×10^{15} atoms/cm^2) of silicon were deposited on the surface from the electron-beam evaporator with a deposition rate of about 0.2 bilayer/sec. The deposition rate was controlled by a quartz-crystal monitor. The LEED picture showed a diffusive background with no spots, confirming that the film was amorphous. STM images of this sample showed a corrugated surface without atomic resolution, which is typical for amorphous silicon.[4,5] The sample was annealed to 430 °C for 10 min to initialize SPE. The LEED picture showed weak (1×1) spots with a diffusive background. The temperature was measured by an infrared pyrometer. The pyrometer was preliminarily calibrated with a Chromel-Alumel thermocouple attached to the back of the sample in a low-gradient furnace. The accuracy of the temperature measurement was estimated as 20 °C.

Figure 1(a) shows a typical STM image of the sample after heating to 430 °C. This image was obtained with a 2-V sample bias voltage and a tunneling current of 1 nA. It is interesting that the surface was changed drastically although the annealing temperature was considerably lower than the reported SPE minimal temperature [the minimal temperature at which the SPE rate is measurable, is about 550 °C (Ref. 3)]. We see that the film is not single crystalline, but consists of (3×3), (5×5), (7×7), and (2×2) reconstructed parts that can be considered as 2–3-nm grains in a polycrystalline film. The film is not homogeneous and contains a number of voids with an average diameter of 3 nm. Such voids were observed before by electron microscopy and their formation was explained as a result of the surface screening by earlier-deposited islands.[13,14] For illustration, Fig. 1(b) shows the STM image of another sample with thickness of amorphous film around 0.5 bilayer after stronger heating

0163-1829/94/50(11)/8020(4)/$06.00

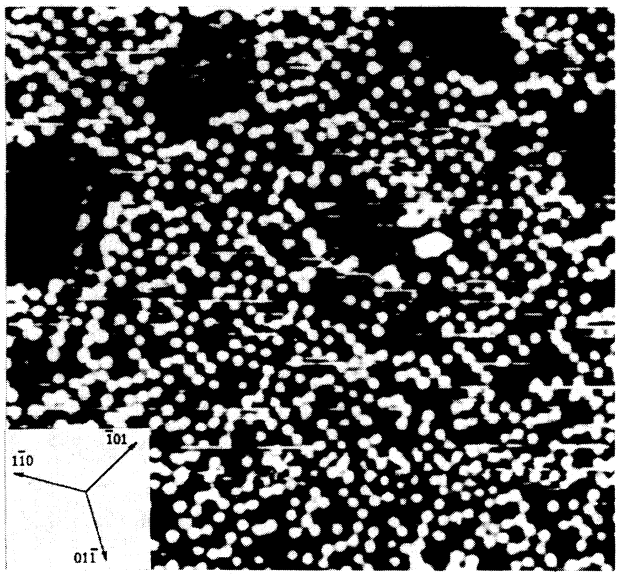

(a)

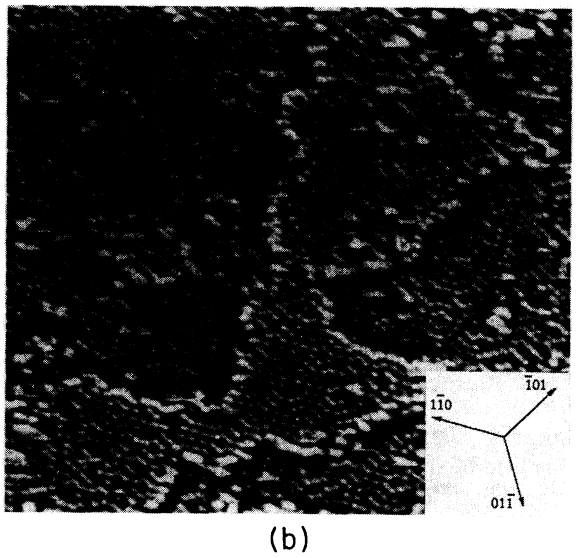

(b)

FIG. 1. STM images of the Si(111) surface covered by an amorphous-silicon layer after annealing. In (a) the thickness of the amorphous film was two bilayers, and the annealing temperature was 430 °C. The area of this image is 29×29 nm^2. In (b) the thickness of the amorphous film was 0.5 bilayers and the annealing temperature was 650 °C. The area of this image is 42×42 nm^1.

(650 °C) for 10 min. The average grain size is larger as a result of coalescence. (5×5), (7×7), and (9×9) reconstructed domains are seen in the central island. This image shows a larger degree of order than the one in Fig. 1(a), confirming that the ordering process can be studied with an atomic resolution at different crystallization stages.

To characterize the order in a quantitative way, we measured the lateral coordinates of the atoms and calculated pair distribution functions $g(r)$ and $G(\mathbf{r})$. Protrusions in the STM images were interpreted as atom locations. Strictly speaking, local density of states should be preliminarily calculated for an accurate determination of the atomic locations. At the moment, this calculation is a formidable task for disordered surfaces.[15] However, an approach of Feenstra[16] can be used for semiconductor surfaces, allowing one to interpret protrusions as dangling bonds corresponding to adatoms on the Si(111) surface. Note that the surface [Fig. 1(a)] is not fully disordered but consists of small grains, which are parts of well-studied reconstructions. The distances between atoms inside each grain coincide with the corresponding distances for single-crystalline surfaces, confirming the validity of our approach.

The coordinates of atoms were determined for a 20×20-nm^2 area taken from the image [Fig. 1(a)] showing a partly disordered surface (495 atoms), and from a (7×7) image of the same area (696 atoms), both after a rigorous thermal-drift compensation. Figure 2 shows $g(r)$ for the (7×7) reconstructed (a) and the partly disordered (b) surfaces. The nearest-neighbor peak in the $g(r)$ for the (7×7) surface is split to two peaks corresponding to $a\sqrt{3}=0.67$ nm and $2a=0.77$ nm, where $a=0.384$ nm is the lattice parameter of an unreconstructed Si(111) surface. Such a splitting is no longer visible in the $g(r)$ for the partly disordered surface, due to the larger degree of disorder at the first coordinate shell. In addition, one can see characteristic peaks for the (7×7) case at 2.7 and 5.4 nm corresponding to the sizes of one and two unit cells, respectively. A comparison with $g(r)$ from a simulated (7×7) surface (not shown here) indicates that the thermal drift was corrected to the extent that it does not perturb the pair distribution function even in large distances. The pair distribution function for the partly disordered surface has a faster decay and larger peak widths, as expected from the polycrystalline structure of the sample. It is interesting that the pair distribution

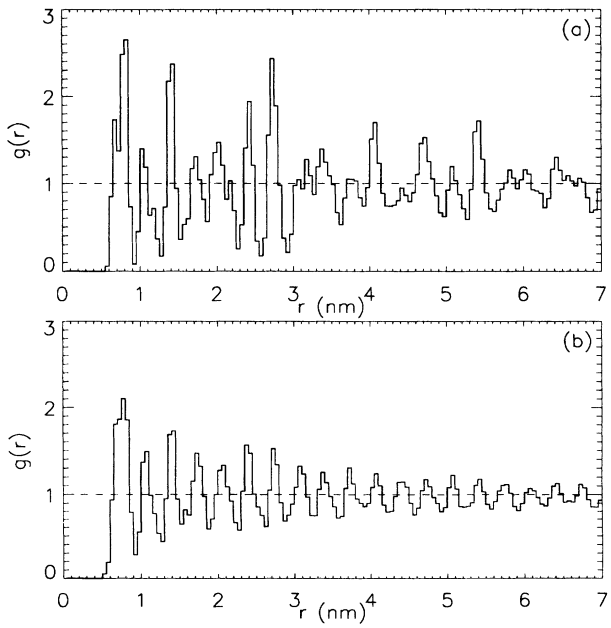

FIG. 2. Pair distribution function $g(r)$ of a 20×20-nm^2 area taken from a (7×7) reconstructed surface (a) and from the partly disordered surface, which is shown in Fig. 1(a).

function does not decay to unity at distances larger than grain size (about 2 nm) but continues to oscillate up to 7 nm with a period of 0.3 nm.

In order to obtain information about orientational order as well, $G(\mathbf{r})$ was calculated. Figure 3 shows nonzero values of $G(\mathbf{r})$ for a (7×7) surface (a) and for the partly disordered surface (b). Every dot in Fig. 3 located a distance $\mathbf{r}$ from the origin means that $G(\mathbf{r})$ is nonzero for this value of $\mathbf{r}$ (i.e., there exists one or more pairs of atoms with this distance). $G(\mathbf{r})$ for the partly disordered surface is a grid with a cell size of 0.384 nm, which is the lattice parameter of the unreconstructed Si(111) surface. It explains the oscillations of $g(r)$ with a period of 0.3 nm at large distances. The grains are commensurate as all atoms are located on the grid. *a*-Si is normally described by the continuous-random-network model[17] and is characterized by bond angle and length distortions (relative to *c*-Si). The grid indicates that the distortions in the partly disordered surface are much smaller. The fact that all the atoms fall on such a grid also confirms *a priori* the determination of atomic coordinates from the STM image.

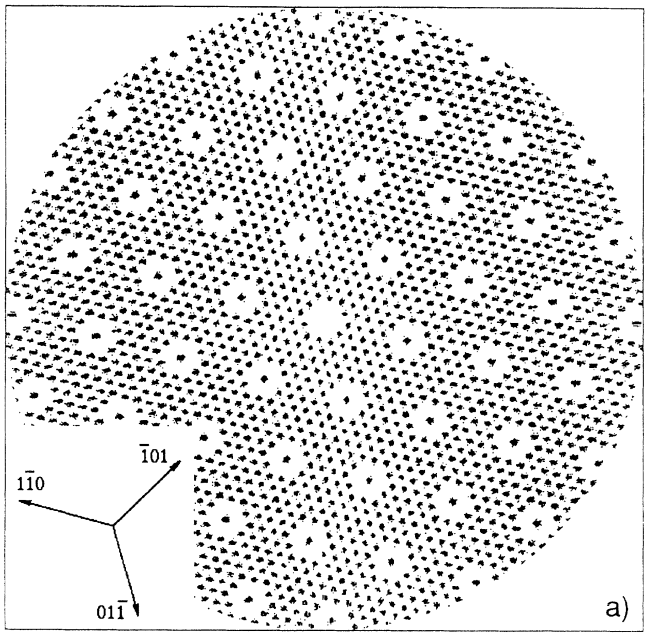

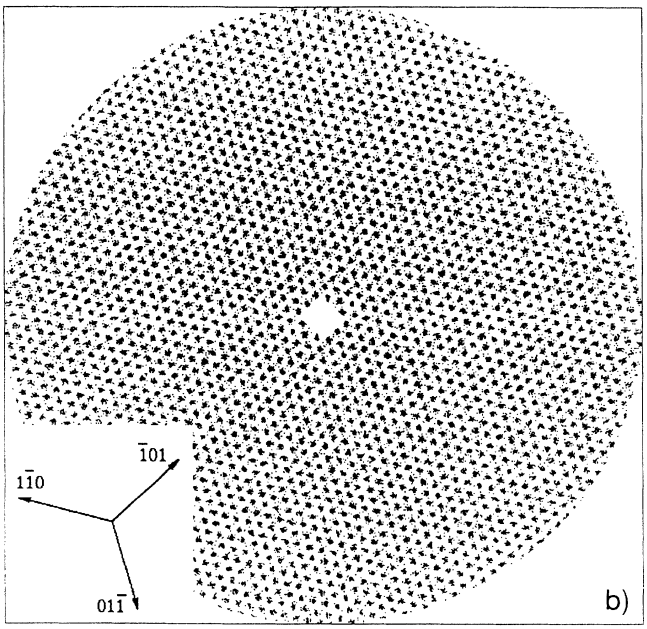

FIG. 3. The pair distribution function $G(\mathbf{r})$ of a 20×20-nm^2 area (7×7) reconstructed surface (a) and the partly disordered surface (b). The largest distance shown in $G(\mathbf{r})$ is 10 nm from the origin located in the center of the image. The absolute values of this function (which might be shown in a gray-scale representation) are not shown for simplicity.

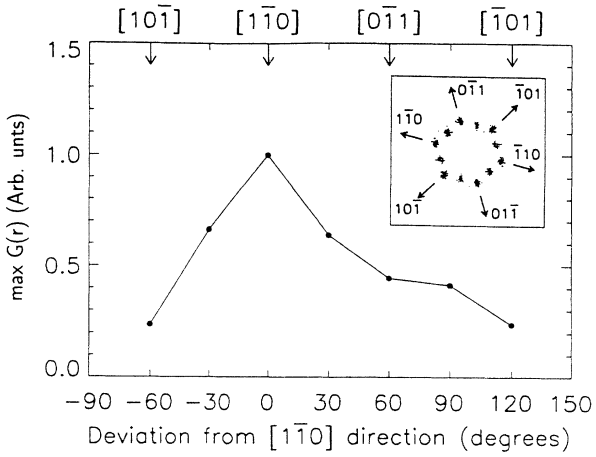

FIG. 4. The maximal values of $G(\mathbf{r})$ for the first-neighbor peaks. The locations of these peaks are shown in the upper-right corner. These peaks correspond to pairs with radial distances of 0.77 and 0.67 nm.

Additional information can be extracted from the absolute values of the peaks in $G(\mathbf{r})$, which are not shown in Fig. 3. The maximum value for the first-neighbor peaks is shown in Fig. 4 for the partly disordered surface. We see that a pronounced maximum exists in the $[1\bar{1}0]$ direction (and a minimum perpendicular to it). It means that the deviation from the ideal crystalline position is smaller in the $[1\bar{1}0]$ direction for the first neighbors. This might indicate that the SPE process is anisotropic with preferable crystallization in the $[1\bar{1}0]$ direction, which is the step direction for the Si(111) surface. This fact is consistent with the Williams and Elliman kink model,[18] considering the SPE process as a movement of kinks along the step. More data should be obtained at different temperatures and in different regions of the surface (e.g., near the step) to observe details of this process.

In conclusion, we observed the SPE of vacuum-deposited amorphous silicon on a Si(111) surface by STM. It was shown that at some conditions atomic resolution can be obtained in the early stages of the SPE process. Lateral coordinates of atoms were extracted. The application of the pair-distribution-function formalism showed that all the atoms are located on a (1×1) grid. Calculation of the two-dimensional pair distribution function revealed the anisotropy of orientational order.

We believe that this fact is a consequence of the anisotropy of the SPE process. The ability to analyze a partly disordered surface in a quantitative way opens many possibilities in following fluctuations and changes in local order. A particularly intriguing possibility is to search for a correlation between the local order and physical quantities that can be measured with the STM, such as surface conductivity or tunneling spectrum.

This work was supported by a grant from the basic research foundation administered by the Israeli Academy of Sciences and Humanities.

[1]L. Csepregi, E. F. Kennedy, J. W. Mayer, and T. W. Sigmon, J. Appl. Phys. **49**, 3906 (1978).
[2]G.-Q. Lu, E. Nygren, and M. J. Aziz, J. Appl. Phys. **70**, 5323 (1991).
[3]G. L. Olson and J. A. Roth, Mater. Sci. Rep. **3**, 1 (1988).
[4]K. Uesugi, T. Yao, T. Sto, T. Sueyoshi, and M. Iwatsuki, Appl. Phys. Lett. **62**, 1600 (1993).
[5]J. Jahanmir, P. E. West, S. Hsieh, and T. N. Rhodin, J. Appl. Phys. **65**, 2064 (1989).
[6]R. S. Becker, B. S. Swartzentruber, J. S. Vickers, and T. Klitsner, Phys. Rev. B **39**, 1633 (1989).
[7]G. Tarrach, R. Wiesendanger, D. Burgler, L. Scandella, and H.-J. Guntherodt, J. Vac. Sci. Technol. B **9**, 677 (1991).
[8]J. Ziman, *Models of Disorder* (Cambridge University Press, Cambridge, 1979).
[9]J. B. Kortright and A. Bienenstock, Phys. Rev. B **37**, 2979 (1988).
[10]H. L. Meyerheim, U. Doebler, A. Puschmann, and K. Baberschke, Phys. Rev. B **41**, 4871 (1990).
[11]C. E. Bouldin, R. A. Forman, M. I. Bell, and E. P. Donovan, Phys. Rev. B **44**, 5492 (1991).
[12]J. E. Demuth, R. J. Hamers, R. M. Tromp, and M. E. Welland, IBM J. Res. Dev. **30**, 396 (1986).
[13]D. K. Pandya, A. C. Rastogi, and K. L. Chopra, J. Appl. Phys. **46**, 2966 (1975).
[14]M. J. J. Theunissen, J. M. L. van Rooij-Mulder, C. W. T. Bulle-Lieuwma, D. E. W. Vandenhoudt, D. J. Gravesteijn, and G. F. A. van de Walle, J. Cryst. Growth **118**, 125 (1992).
[15]J. Tersoff, in *Scanning Tunneling Microscopy and Related Methods,* Vol. 184 of *NATO Advanced Study Institute, Series E: Applied Sciences,* edited by R. J. Behm, N. Garcia, and H. Rohrer (Kluwer, Dordrecht, 1990), p. 84.
[16]R. M. Feenstra, in *Scanning Tunneling Microscopy and Related Methods* (Ref. 15), p. 211.
[17]W. H. Zachariassen, J. Am. Chem. Soc. **54**, 3841 (1932).
[18]J. S. Williams and R. G. Elliman, Phys. Rev. Lett. **51**, 1069 (1983).

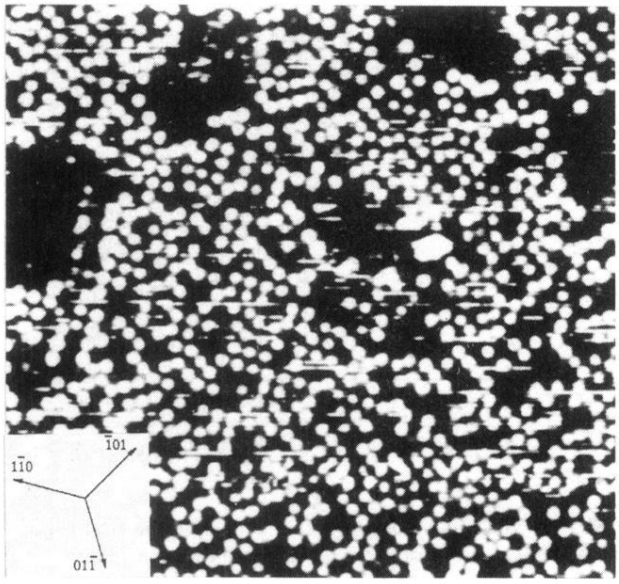

(a)

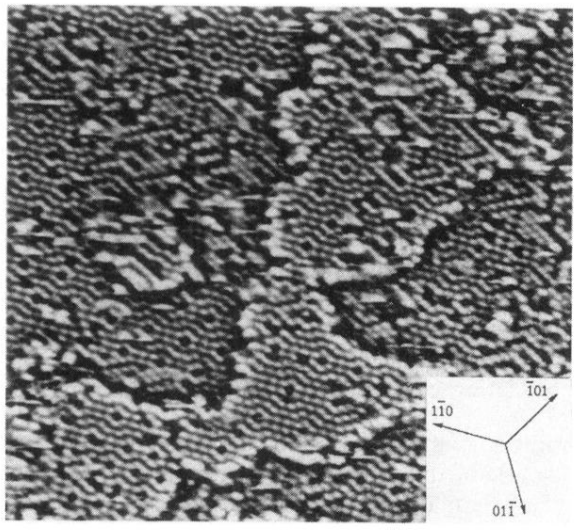

(b)

FIG. 1. STM images of the Si(111) surface covered by an amorphous-silicon layer after annealing. In (a) the thickness of the amorphous film was two bilayers, and the annealing temperature was 430 °C. The area of this image is 29×29 nm^2. In (b) the thickness of the amorphous film was 0.5 bilayers and the annealing temperature was 650 °C. The area of this image is 42×42 nm[1].